

22 **Abstract**

23 Hereditary hemochromatosis (HH) is an autosomal recessive disorder of excess
24 iron absorption. The most common form, HH1, is caused by loss of function variants in
25 *HFE*. *HFE* encodes a cell surface protein that binds to the Transferrin Receptor (TfR1),
26 reducing TfR1's affinity for the transferrin/iron complex and thereby limiting cellular
27 iron uptake. Two common missense alleles for HH1 have been identified, *HFE* C282Y
28 and *HFE* H63D; H63D is considered to be a less penetrant allele. When we deployed
29 Phenotype Risk Scores (PheRS), a method that aggregates multiple symptoms together in
30 Electronic Health Records (EHRs), we identified *HFE* E168Q as a novel variant
31 associated with HH. E168Q is on the same haplotype as H63D, and in a crystal structure
32 *HFE* E168 lies at the interface of the HFE-TfR1 interaction and makes multiple salt
33 bridge connections with TfR1. In *in vitro* cell surface abundance experiments, the *HFE*
34 E168Q+H63D double mutation surprisingly increased cell surface abundance of HFE by
35 10-fold compared to wildtype. In coimmunoprecipitation experiments, however, HFE
36 C282Y, E168Q, and E168Q+H63D completely abolished the interaction between HFE
37 and TfR1, while H63D alone only partially reduced binding. These findings provide
38 mechanistic insight to validate the PheRS result that *HFE* E168Q is an HH1-associated
39 allele and lead to the reclassification of E168Q from a variant of uncertain significance to
40 a pathogenic variant, according to ACMG guidelines. *HFE* E168Q results in loss of HFE
41 function by disrupting the HFE-TfR1 interaction. In addition, some disease
42 manifestations attributed to H63D may reflect the functional effects of E168Q.

43

44

45 **Introduction**

46 Hereditary hemochromatosis (HH) is a genetic disorder in which the body absorbs
47 excess iron.¹ The excess iron can cause damage to the body's tissues, resulting in a
48 myriad of symptoms, sometimes culminating in liver failure, heart failure, or diabetes.
49 HH has been linked to variants in multiple genes, including autosomal recessively
50 inherited variants in *HFE* (Hemochromatosis Type 1, HH1 [MIM 235200]). Two classic
51 common risk alleles for HH1 in *HFE* are C282Y and H63D.^{2,3} These missense variants
52 are common, with minor allele frequencies of 0-6% and 2-15% respectively, depending
53 on ancestry.⁴ C282Y homozygotes are considered to have the highest risk for HH, with
54 C282Y heterozygotes, H63D homozygotes, and C282Y/H63D compound heterozygotes
55 at lower risk.^{5,6}

56 *HFE* is a 343 amino acid single-pass transmembrane protein with a large
57 extracellular domain. The extracellular domain of *HFE* binds the extracellular domain of
58 Transferrin Receptor 1 (TfR1), reducing the affinity of TfR1 for transferrin. When *HFE*
59 is unable to bind TfR1 sufficiently, TfR1 has increased affinity for transferrin, resulting
60 in excess iron uptake into cells and hemochromatosis. C282Y eliminates a disulfide bond
61 in the extracellular domain of *HFE*, causing misfolding of *HFE* and failure to traffic to
62 the cell surface.³ H63D is thought to cause HH by having a smaller effect on reducing the
63 affinity of TfR1 for transferrin.² Several additional rare variants have been observed in
64 patients with HH in the literature, typically as compound heterozygotes with C282Y or
65 H63D.⁷⁻⁹

66 A promising method to evaluate the risk of genetic variants is in environments
67 that have relatively unselected populations with available Electronic Health Record

68 (EHR) data and genotypic data. Recently, we have developed Phenotype Risk Scores
69 (PheRS) as a method to analyze syndromic phenotypes that have a range of phenotypic
70 effects and to link novel variants. The first deployment of PheRS in a biobank population
71 identified 18 associations between SNPs and syndromic diseases.¹⁰ One of the
72 associations was between *HFE* E168Q (c.502G>C) and hemochromatosis risk score. Out
73 of the 40 heterozygous carriers of *HFE* E168Q, 8 had highly elevated PheRS's for HH,
74 and 4 had received a liver transplant. However, whether E168Q actually alters *HFE*
75 function remains unclear. Largely due to the lack of *in vitro* functional data about its
76 mechanism, E168Q is still classified as a variant of uncertain significance.¹⁰

77 Here we investigate the function of *HFE* E168Q using *in vitro* functional assays.
78 We find that E168Q is located on the same haplotype as H63D, and that E168Q+H63D
79 has increased abundance at the cell surface. E168Q lies at the interface of the *HFE*-TfR1
80 interaction and completely disrupts that interaction, establishing a mechanism for
81 E168Q's association with hemochromatosis.

82

83 **Material and Methods**

84 Haplotype analysis

85 52,573 adult (>18 years) individuals of European ancestry were included in the analysis.

86 These individuals were genotyped with the Multi-Ethnic Global Array (Illumina) or the
87 Infinium HumanExome BeadChip array (Illumina). Genotypes were determined for *HFE*
88 H63D (rs1799945) or *HFE* E168Q (rs146519482). Ancestry was determined from
89 STRUCTURE.¹¹

90

91 Mutagenesis and Transfection

92 pCB6-HFE-EGFP was a gift from Pamela Bjorkman (Addgene plasmid # 12104). This
93 plasmid was mutated with a Quikchange Lightning Multi-site kit (Agilent) to create
94 C282Y, H63D, E168Q, and E168Q+H63D mutant plasmids. Plasmids were transfected
95 into HeLa, HepG2, Chinese Hamster Ovary, or HEK293 cells using Fugene 6 (Promega)
96 following manufacturer's instructions and studied 48-72 hours post-transfection.

97

98 Cell surface abundance assays

99 To stain cells for confocal and flow cytometry experiments, HeLa, HepG2, HEK293, or
100 CHO cells were stained with an anti-HFE antibody while still alive—thus, having an
101 intact cell membrane—to quantify HFE at the cell surface. Briefly, cells transfected with
102 wildtype or mutant *HFE*-GFP (see above) were trypsinized, resuspended in complete
103 media, washed in PBS+1%Bovine Serum Albumin, incubated with a polyclonal anti-
104 HFE antibody at 1:500 dilution (ThermoFisher PA5-37364), washed twice in PBS+BSA,
105 incubated with a Alexa Fluor 647-anti-rabbit secondary antibody at 1:500 (ThermoFisher
106 A-21245), and washed twice in PBS+BSA. For flow cytometry, cells were analyzed on a
107 BD LSR Fortessa instrument, using a 488 nm laser and 525/50 nm filter for GFP, and a
108 633 nm laser and 660/20 filter for Alexa Fluor 647. Single cells were identified from side
109 and forward scatter parameters, and GFP and Alexa Fluor 647 laser levels were set so
110 that untransfected cells had a median of 100 for each. Cells with a high level of GFP were
111 identified (cells with ~100-fold GFP levels relative to wildtype; $10^{1.8}$ to $10^{2.2}$ -fold
112 higher). The median Alexa Fluor 647 level of highly-GFP+ cells was calculated and
113 averaged across at least 3 replicate samples. Statistical analyses were performed in R.

114 Student's two tailed t-tests were used for comparisons between groups. For confocal
115 microscopy, cells were stained as above, fixed with 4% paraformaldehyde, washed with
116 PBS+Hoechst, and imaged on an Olympus FV-1000 confocal microscope using identical
117 settings for each mutation.

118

119 Co-Immunoprecipitation

120 HeLa cells were chosen for coimmunoprecipitation experiments because wildtype HFE
121 trafficked best to the cell surface in HeLa cells (Figure S1) and they had been previously
122 used for coimmunoprecipitation experiments.⁹ HeLa cells were cotransfected using
123 Fugene 6 with wildtype or mutant *HFE*-GFP plasmids (see above) and a Transferrin
124 Receptor 1 expression plasmid pcDNA3.2/DEST/hTfR-HA, a gift from Robin Shaw
125 (Addgene plasmid #69610). A Pierce Classic Magnetic IP/Co-IP Kit (ThermoFisher
126 #88804) was used to harvest and coimmunoprecipitate the cells, following
127 manufacturer's instructions. Cells were precipitated with a rabbit anti-GFP antibody
128 (AbCam #ab290), then Western blots were performed using the anti-GFP antibody
129 (1:2500) or a mouse anti-TfR1 antibody (ThermoFisher #13-6800, 1:500) or a secondary
130 anti-rabbit HRP (Promega #W4011) and anti-mouse HRP (Promega W-4021) antibody,
131 each at 1:10,000.

132

133 Variant classification

134 *HFE* E168Q was classified according to American College of Medical Genetics and
135 Genomics criteria,¹² which integrates multiple variables into a benign/likely
136 benign/uncertain significance/likely pathogenic/pathogenic classification. The University

137 of Maryland Genetic Variant Interpretation Tool was used to implement these criteria
138 (medschool.umaryland.edu/Genetic_Variant_Interpretation_Tool1.html).¹³

139

140 **Results**

141 *HFE* E168Q is a rare allele on the same haplotype as H63D

142 *HFE* E168Q was previously shown using PheRS to have an association with
143 hemochromatosis.¹⁰ When we examined *HFE* genotypes of E168Q heterozygotes, we
144 observed that E168Q cosegregated with the common H63D allele (88/88 E168Q
145 heterozygotes had at least 1 H63D allele; Table 1). In individuals with European
146 ancestry, E168Q had a minor allele frequency of 0.00084 and H63D had a minor allele
147 frequency of 0.149. E168Q was exclusively present in individuals of European ancestry,
148 except for 1 individual whose ancestry was undetermined by STRUCTURE, and is likely
149 of mixed ancestry. 13 of the 88 E168Q heterozygotes (14.7%) were homozygous for
150 H63D, similar to the minor allele frequency of H63D, indicating that these individuals
151 were likely E168Q+H63D / H63D compound heterozygotes. Together, these data
152 indicate that E168Q is a rare variant that arose on the H63D allele of *HFE*.

153

154 *HFE* E168Q+H63D has increased abundance at the cell surface

155 A common mechanism for loss of function of membrane proteins is a defect in
156 trafficking to the cell surface, often due to misfolding of the protein and subsequent
157 aggregation along the secretory pathway.¹⁴ Cell surface abundance can also be affected
158 by altered rates of internalization or degradation. We developed a dual flow cytometry
159 and confocal microscopy-based assay to assay the subcellular localization of a GFP-

160 tagged HFE protein. Testing of four cell lines (HeLa, HepG2, Chinese Hamster Ovary,
161 and HEK293) revealed that wildtype HFE trafficking efficiency varied widely between
162 cell lines, trafficking best in HeLa cells, followed by HepG2 cells (Figure S1). To test
163 whether mutant HFE proteins were present in different abundances at the cell surface, we
164 examined the cellular localization of GFP-tagged HFE wildtype protein and HFE mutants
165 H63D, E168Q, C282Y, and the E168Q+H63D double mutant (hereafter referred to as
166 E168Q+H63D) (Figure 1). C282Y showed a dramatic trafficking defect (5% of wildtype
167 level, $p=3.2e-5$, two-tailed T test). E168Q had a mild but significant increase in surface
168 abundance (136% of wildtype level, $p=0.01$). H63D surprisingly had a higher abundance
169 than wildtype (722% of wildtype level, $p=0.02$). E168Q+H63D also had a large increase
170 in surface abundance (970% of wildtype level, $p=0.02$). Similar relative surface
171 abundance results were observed in the HepG2 liver cell line, albeit with lower overall
172 levels of surface trafficking (Figures 1, S1). Therefore, in contrast to C282Y, H63D and
173 H63D+E168Q have increased cell surface abundances.

174

175 HFE E168 is at the interface of the HFE-Transferrin Receptor interaction

176 We next examined the location of E168Q within the HFE protein. A crystal
177 structure of the HFE-TfR1 interaction has been solved, together with the HFE binding
178 partner B2M (Figure 2).¹⁵ That crystal structure revealed six residues of HFE that made
179 salt bridges with TfR1 (Table S1). Intriguingly, in the structure, one of these residues is
180 HFE E168, which is located at the HFE-TfR1 interface, and makes salt bridges with two
181 TfR1 residues (TfR1-R629 and TfR1-Q640). HFE E168Q is also predicted to make an
182 intramolecular salt bridge with HFE N108.

183

184 HFE E168Q disrupts the interaction between HFE and the Transferrin Receptor

185 Because of HFE E168's location and contacts with TfR1, we hypothesized that
186 the HFE E168Q variant disrupts the binding between HFE and TfR1. To test this, we
187 performed coimmunoprecipitation experiments, precipitating HFE-GFP using an anti-
188 GFP antibody and measuring coimmunoprecipitation of TfR1 (Figure 3). Wildtype HFE-
189 GFP coimmunoprecipitated TfR1, but C282Y, E168Q, and E168Q+H63D showed no
190 coimmunoprecipitation of TfR1. Across multiple replicates, C282Y had lower overall
191 intensity of anti-GFP staining in both input and immunoprecipitated samples, consistent
192 with a previously observed accelerated degradation rate of this variant.³ H63D showed a
193 detectable but decreased coimmunoprecipitation of TfR1. Thus, E168Q and
194 E168Q+H63D had a more severe defect in binding TfR1 than H63D.

195

196 Pathogenicity reclassification of *HFE* E168Q

197 We used American College of Medical Genetics and Genomics criteria to
198 determine the classification of *HFE* E168Q using data available before this study and
199 after this study (Table 2). Despite the genetic association in a biobank population, *HFE*
200 E168Q before this study was still classified as a variant of uncertain significance based
201 on criterion PS4 (variant prevalence in affected individuals is significantly increased
202 compared with the prevalence in controls).¹⁰ Based on the updated *in vitro* functional data
203 in this paper (criteria PS3), *HFE* E168Q now has enough evidence to be classified as a
204 pathogenic variant.

205

206 **Discussion**

207 Phenotype Risk Scores for syndromic traits

208 *HFE* E168Q was identified as a novel HH1 allele with PheRS, a recently
209 developed method that combines multiple phenotypes into a weighted score, to study the
210 HH risk of different *HFE* variants. The PheRS for hemochromatosis includes 22
211 symptoms, such as liver cirrhosis, hepatic cancer, cardiac dysrhythmias, and type 2
212 diabetes. The *in vitro* work presented here validating E168Q as a loss of function allele
213 validates the use of PheRS as a powerful way to assess the disease risk of variants. As the
214 number of individuals in EHR datasets linked to genotyping grows, this approach will
215 gain in power to detect genetic associations. Given the size of contemporary biobanks
216 linking DNA variation to human phenotypes,¹⁶ this approach will likely prove fruitful for
217 rare but not ultrarare variants such as E168Q (minor allele frequency of 0.08% in
218 Europeans) that are still present in many individuals in large biobanks. However, for
219 some variants like *HFE* E168Q, statistical association in biobanks is not enough to
220 classify variants as pathogenic or likely pathogenic, and further *in vitro* functional
221 validation is required. The combination of statistical association by PheRS and *in vitro*
222 loss of function phenotype is enough to reclassify *HFE* E168Q as pathogenic.

223

224 Mechanism of *HFE* E168Q

225 A main mechanism of transmembrane proteins having loss of function is
226 misfolding and subsequent failure to traffic to the cell membrane. However, in this work,
227 we surprisingly observed that *HFE* E168Q+H63D had increased abundance at the cell
228 surface. Much of this surface abundance difference was due to H63D, although E168Q

229 alone had a mild but significant increase in surface abundance. We observed that HFE
230 E168 was at the interface of the HFE-TfR1 interaction and made multiple salt bridge
231 contacts with TfR1, suggesting that E168Q would disrupt the salt bridge contacts with
232 TfR1. Indeed, coimmunoprecipitation experiments showed a complete loss of binding of
233 E168Q and E168Q+H63D. Although it is difficult to predict the exact configuration of
234 the mutant glutamine in the crystal structure, the glutamine likely completely disrupts the
235 interaction between HFE-168 and TfR1-R629 and likely alters the contacts with TfR1-
236 Q640. Two main alpha helices make contact with TfR1, termed $\alpha 1$ and $\alpha 2$.¹⁵ HFE E168
237 is located in $\alpha 2$. Previous work showed that mutation to alanine of two residues in $\alpha 1$,
238 V100 and W103 (called V78 and W81 in the original paper), also abrogated the binding
239 between HFE and TfR1.¹⁷ Therefore, we propose a model in which *HFE* E168Q is unable
240 to bind TfR1 and TfR1 therefore has an increased affinity for transferrin, causing iron
241 overload and HH1.

242

243 Improved prediction of HH risk

244 Our results suggest a template for improved prediction of HH risk. Our results
245 further suggest that genotyping for H63D and C282Y alone might not be sufficient to
246 determine HH1 risk. H63D is considered to be a low/variable penetrance HH1 allele,^{5,6}
247 and E168Q presence may underlie some of the HH1 risk previously attributed to H63D
248 alone and explain some of its variable penetrance.¹⁸ Other rare HFE variants in $\alpha 1$ and $\alpha 2$
249 or making salt bridge connections with TfR1 may also disrupt TfR1 binding and lead to
250 hemochromatosis. Integrated phenotyping methods like PheRS show promise to identify
251 risk variants and may also identify patients with underrecognized disease. However,

252 further functional studies are often necessary to validate these variants; 9/18 variants in
253 the initial PheRS paper were classified as variants of uncertain significance despite their
254 statistical association with disease.¹⁰ *In vitro* functional studies such as the surface
255 abundance and coimmunoprecipitation studies in this paper can validate the genetic
256 results and result in reclassification of variants as benign or pathogenic. We anticipate
257 that these methods will be more broadly applied to other variants, genes, and diseases to
258 better predict disease risk.

259 **Supplemental Data Description**

260

261 The Supplemental Data contains 1 figure and 1 table.

262

263 Figure S1. HFE traffics robustly to the cell membrane in HeLa cells

264 Table S1. Residues of HFE forming salt bridges with TfR1

265

266

267 **Declaration of Interests**

268 The authors declare no competing interests.

269

270 **Acknowledgements**

271 This work was supported by grants R01-LM010685 from the National Library of
272 Medicine and P50-GM115305 from the National Institute for General Medical Sciences
273 and a grant from the Robert J. Kleberg, Jr. and Helen C. Kleberg Foundation. BioVU
274 received and continues to receive support through the National Center for Research
275 Resources (UL1-RR024975), which is now the National Center for Advancing
276 Translational Sciences (UL1-TR000445). A.M.G. was supported by F32 HL137385 and
277 T32 HG008341. B.M.K. was supported by K99 HL135442.

278

279 **Figure Legends**

280

281 **Figure 1: HFE E168Q+H63D has enhanced surface abundance**

282 HeLa or HepG2 cells were transfected with *HFE*-GFP and stained while alive for HFE at
283 the cell surface (Alexa Fluor 647). A) Representative confocal microscopic images of
284 HeLa cells (blue=Hoechst nuclear stain, green=GFP, red=Alexa Fluor 647). B)
285 Representative flow cytometry plots of surface HFE staining in HeLa cells. Red box
286 indicates transfected cells (GFP+ 100-fold higher than untransfected cells). X and Y-axis
287 scales are in \log_{10} units. C-D) Quantification of flow cytometry data of cell surface
288 staining in HeLa (C) or HepG2 (D) cells (mean + SEM). Values are normalized to the
289 mean wildtype level. * $p < 0.05$, ** $p < 0.005$, two-tailed T test. C) $n = 5-6$ replicate
290 samples/mutation. D) $n = 3$ replicate samples/mutation.

291

292 **Figure 2: HFE E168 is located at the interface of the HFE-TfR1 interaction**

293 A) Schematic of HFE/TfR1/B2M interactions at the cell surface. Orange/yellow rectangle
294 indicates plasma membrane. B-D) Crystal structure of HFE-TfR1-B2M extracellular
295 domains.¹⁵ HFE is colored in salmon, TfR1 in green, B2M in blue. Each protein is present
296 twice in the complex, but only one instance is colored, and the other instance is shown in
297 gray. B) Side view. C) Top view with zoom. Salt bridges between HFE E168 and HFE
298 N108, TfR1 R629, and TfR1 Q640 are shown with dotted lines.

299

300 **Figure 3: HFE E168Q disrupts the interaction between HFE and the Transferrin**

301 **Receptor**

302 Coimmunoprecipitation experiments. A) Input. B) HFE-GFP was immunoprecipitated
303 with an anti-GFP antibody. For A and B, Western blots using anti-GFP or anti-TfR1 are
304 shown. Similar results were observed across 3 replicate experiments.

305

306

307 **Table 1: E168Q is a rare variant on the same haplotype as H63D**

308

	H63D allele		
E168Q allele	HH	HD	DD
EE	38,084	13,256	1,145
EQ	0	75	13
QQ	0	0	0

309

310 Co-occurrence of *HFE* H63D and E168Q genotypes in 52,573 adult European-ancestry

311 individuals. The 168Q allele only appears in the presence of the 63D allele, indicating

312 that the 168Q allele is on the same haplotype as the 63D allele.

313

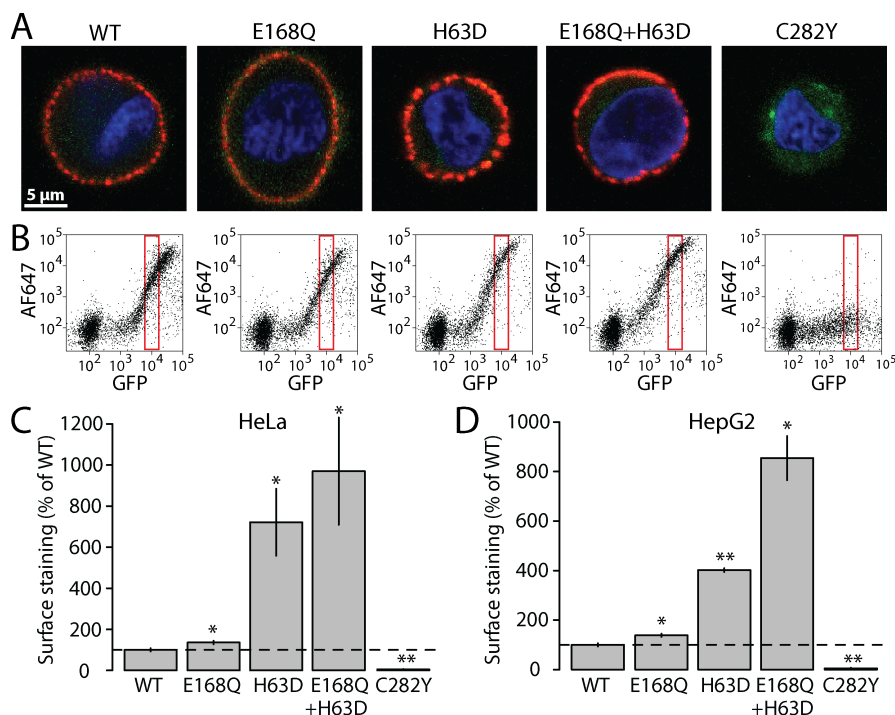
314

315

316

317 **Figure 1: HFE E168Q+H63D has enhanced trafficking to the cell surface**

318



319

320

321 HeLa or HepG2 cells were transfected with *HFE*-GFP and stained while alive for HFE at

322 the cell surface (Alexa Fluor 647). A) Representative confocal microscopic images of

323 HeLa cells (blue=Hoechst nuclear stain, green=GFP, red=Alexa Fluor 647). B)

324 Representative flow cytometry plots of surface HFE staining in HeLa cells. Red box

325 indicates transfected cells (GFP+ 100-fold higher than untransfected cells). X and Y-axis

326 scales are in log₁₀ units. C-D) Quantification of flow cytometry data of cell surface

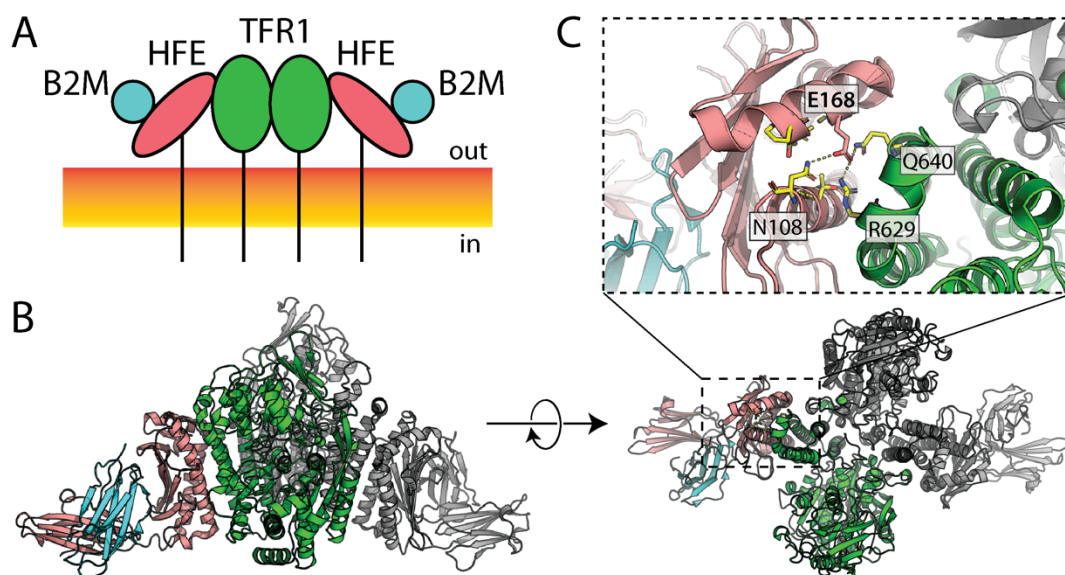
327 staining in HeLa (C) or HepG2 (D) cells. Values are normalized to the mean wildtype

328 level. *p<0.05, **p<0.005, two-tailed T test. C) n=5-6 replicate samples/mutation. D)

329 n=3 replicate samples/mutation.

330 **Figure 2: HFE E168 is located at the interface of the HFE-TfR1 interaction**

331



332

333

334

335

336 A) Schematic of HFE/TfR1/B2M interactions at the cell surface. Orange/yellow rectangle

337 indicates plasma membrane. B-D) Crystal structure of HFE-TfR1-B2M extracellular

338 domains.¹⁵ HFE is colored in salmon, TfR1 in green, B2M in blue. Each protein is present

339 twice in the complex, but only one instance is colored, and the other instance is shown in

340 gray. B) Side view. C) Top view with zoom. Salt bridges between HFE E168 and HFE

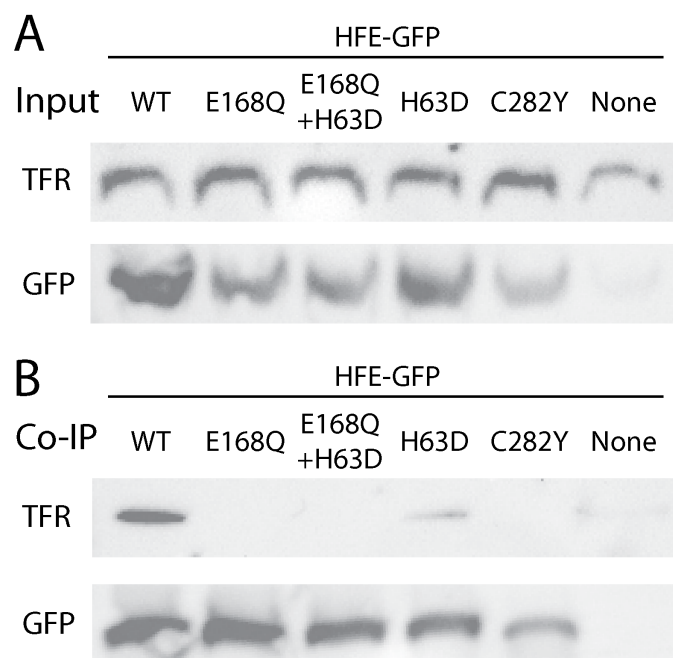
341 N108, TfR1 R629, and TfR1 Q640 are shown with dotted lines.

342

343 **Figure 3: HFE E168Q disrupts the interaction between HFE and the Transferrin**

344 **Receptor**

345



346

347

348 Coimmunoprecipitation experiments. A) Input. B) HFE-GFP was immunoprecipitated

349 with an anti-GFP antibody. For A and B, Western blots using anti-GFP or anti-TfR1 are

350 shown. Similar results were observed across 3 replicate experiments.

351

352

353 **Table 2. Classification of HFE E168Q using ACMG guidelines**

354

ACMG Criterion	Description	Before this study	After this study
PS3	Well-established <i>in vitro</i> or <i>in vivo</i> functional studies supportive of a damaging effect on the gene or gene product	No	Yes
PS4	Variant prevalence in affected individuals is significantly increased compared with the prevalence in controls	Yes	Yes
Classification		VUS	Pathogenic

355

356 American College of Medical Genetics and Genomics (ACMG) classification

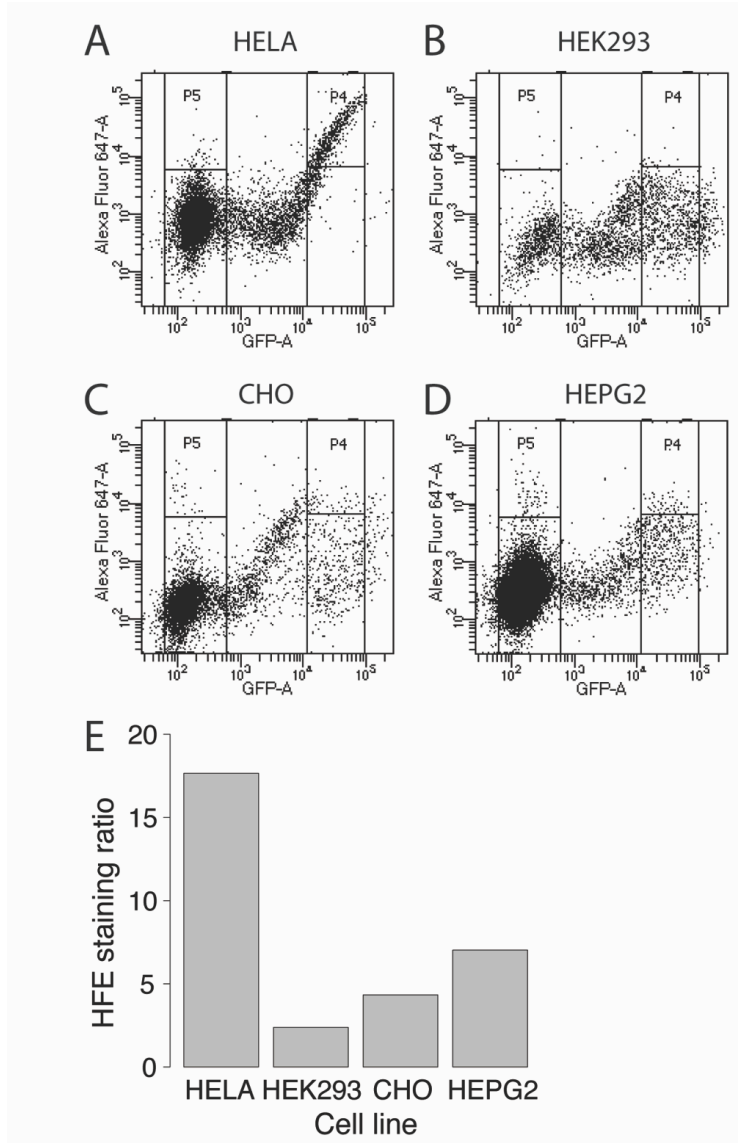
357 guidelines¹² were implemented using the online Genetic Variant Interpretation Tool.¹³

358 Because of the *in vitro* functional evidence in this study, the classification of E168Q

359 changed from Variant of Uncertain Significance (VUS) to Pathogenic.

360

361 **Figure S1. HFE traffics robustly to the cell membrane in HeLa cells**
362



363

364

365

366 A-D) Wildtype HFE cell surface staining (Alexa Fluor 647) vs. HFE-GFP level (GFP) in

367 transiently transfected HeLa (A), HEK293 (B), CHO (C), or HepG2 cells (D). E) A HFE

368 staining ratio was calculated by taking the median Alexa Fluor 647 level in highly

369 expressing cells (P4) divided by the median Alexa Fluor 647 level in untransfected cells

370 (P5).

371 **Table S1. Residues of HFE forming salt bridges with Tfr1**

372

HFE residue (contemporary numbering)	HFE residue (Bennett <i>et al.</i> numbering)	HFE location	Interacting Tfr1 residue
Gln86	Gln64	α 1 helix	Thr658
Glu107	Glu85	α 1 helix	Arg629
Asn108	Asn86	α 1 helix	Arg629
Glu168	Glu146	α 2 helix	Arg629, Gln640
Arg175	Arg153	α 2 helix	Gln640
Gln178	Gln156	α 2 helix	Asp648

373

374 Table adapted from Bennett *et al.* 2000.¹⁵

375

Literature Cited

376

377

- 378 1. Powell LW, Seckington RC, Deugnier Y. Haemochromatosis. *Lancet*.
379 2016;388:706-716. PMID: WOS:000381268700031.
- 380 2. Feder JN, Gnirke A, Thomas W, Tsuchihashi Z, Ruddy DA, Risch NJ, Bacon BR,
381 Wolff RK. A novel MHC class I-like gene is mutated in patients with
382 hemochromatosis. *Blood*. 1996;88:2579-2579. PMID:
383 WOS:A1996VT98302579.
- 384 3. Waheed A, Parkkila S, Zhou XY, Tomatsu S, Tsuchihashi Z, Feder JN,
385 Schatzman RC, Britton RS, Bacon BR, Sly WS. Hereditary hemochromatosis:
386 Effects of C282Y and H63D mutations on association with beta(2)-
387 microglobulin, intracellular processing, and cell surface expression of the
388 HFE protein in COS-7 cells. *P Natl Acad Sci USA*. 1997;94:12384-12389.
389 PMID: WOS:A1997YF39300027.
- 390 4. Lek M, Karczewski KJ, Minikel EV, Samocha KE, Banks E, Fennell T,
391 O'Donnell-Luria AH, Ware JS, Hill AJ, Cummings BB, Tukiainen T, Birnbaum
392 DP, Kosmicki JA, Duncan LE, Estrada K, Zhao F, Zou J, Pierce-Hoffman E,
393 Berghout J, Cooper DN, Deflaux N, DePristo M, Do R, Flannick J, Fromer M,
394 Gauthier L, Goldstein J, Gupta N, Howrigan D, Kiezun A, Kurki MI, Moonshine
395 AL, Natarajan P, Orozco L, Peloso GM, Poplin R, Rivas MA, Ruano-Rubio V,
396 Rose SA, Ruderfer DM, Shakir K, Stenson PD, Stevens C, Thomas BP, Tiao G,
397 Tusie-Luna MT, Weisburd B, Won HH, Yu D, Altshuler DM, Ardissino D,
398 Boehnke M, Danesh J, Donnelly S, Elosua R, Florez JC, Gabriel SB, Getz G, Glatt
399 SJ, Hultman CM, Kathiresan S, Laakso M, McCarroll S, McCarthy MI, McGovern
400 D, McPherson R, Neale BM, Palotie A, Purcell SM, Saleheen D, Scharf JM, Sklar
401 P, Sullivan PF, Tuomilehto J, Tsuang MT, Watkins HC, Wilson JG, Daly MJ,
402 MacArthur DG, Exome Aggregation C. Analysis of protein-coding genetic
403 variation in 60,706 humans. *Nature*. 2016;536:285-291. PMID: 27535533.
404 PMID: PMC5018207
- 405 5. Allen KJ, Gurrin LC, Constantine CC, Osborne NJ, Delatycki MB, Nicoll AJ,
406 McLaren CE, Bahlo M, Nisselle AE, Vulpe CD, Anderson GJ, Southey MC, Giles
407 GG, English DR, Hopper JL, Olynyk JK, Powell LW, Gertig DM. Iron-overload-
408 related disease in HFE hereditary hemochromatosis. *N Engl J Med*.
409 2008;358:221-230. PMID: 18199861.
- 410 6. Beutler E, Felitti VJ, Koziol JA, Ho NJ, Gelbart T. Penetrance of 845G--> A
411 (C282Y) HFE hereditary haemochromatosis mutation in the USA. *Lancet*.
412 2002;359:211-218. PMID: 11812557.
- 413 7. Aguilar-Martinez P, Grandchamp B, Cunat S, Cadet E, Blanc F, Nourrit M,
414 Lassoued K, Schved JF, Rochette J. Iron overload in HFE C282Y heterozygotes
415 at first genetic testing: a strategy for identifying rare HFE variants.
416 *Haematologica*. 2011;96:507-514. PMID: 21228038. PMID: PMC3069226
- 417 8. Cezard C, Rabbind Singh A, Le Gac G, Gourlaouen I, Ferec C, Rochette J.
418 Phenotypic expression of a novel C282Y/R226G compound heterozygous
419 state in HFE hemochromatosis: molecular dynamics and biochemical studies.
420 *Blood Cells Mol Dis*. 2014;52:27-34. PMID: 23953397.

- 421 9. Silva B, Martins R, Proenca D, Fleming R, Faustino P. The functional
422 significance of E277K and V295A HFE mutations. *Br J Haematol*.
423 2012;158:399-408. PMID: 22624560.
- 424 10. Bastarache L, Hughey JJ, Hebring S, Marlo J, Zhao WK, Ho WTT, Van Driest
425 SL, McGregor TL, Mosley JD, Wells QS, Temple M, Ramirez AH, Carroll R,
426 Osterman T, Edwards T, Ruderfer D, Edwards DRV, Hamid R, Cogan J, Glazer
427 A, Wei WQ, Feng QP, Brilliant M, Zhao ZZJ, Cox NJ, Roden DM, Denny JC.
428 Phenotype risk scores identify patients with unrecognized Mendelian disease
429 patterns. *Science*. 2018;359:1233-+. PMID: WOS:000427504900035.
- 430 11. Pritchard JK, Stephens M, Donnelly P. Inference of population structure using
431 multilocus genotype data. *Genetics*. 2000;155:945-959. PMID:
432 WOS:000087475100039.
- 433 12. Richards S, Aziz N, Bale S, Bick D, Das S, Gastier-Foster J, Grody WW, Hegde
434 M, Lyon E, Spector E, Voelkerding K, Rehm HL, Committee ALQA. Standards
435 and guidelines for the interpretation of sequence variants: a joint consensus
436 recommendation of the American College of Medical Genetics and Genomics
437 and the Association for Molecular Pathology. *Genet Med*. 2015;17:405-424.
438 PMID: 25741868. PMCID: PMC4544753
- 439 13. Kleinberger J, Maloney KA, Pollin TI, Jeng LJ. An openly available online tool
440 for implementing the ACMG/AMP standards and guidelines for the
441 interpretation of sequence variants. *Genet Med*. 2016;18:1165. PMID:
442 26986878. PMCID: PMC5026899
- 443 14. Schleich JP, Sanders CR. The safety dance: biophysics of membrane protein
444 folding and misfolding in a cellular context. *Q Rev Biophys*. 2015;48:1-34.
445 PMID: 25420508. PMCID: PMC4339315
- 446 15. Bennett MJ, Lebron JA, Bjorkman PJ. Crystal structure of the hereditary
447 haemochromatosis protein HFE complexed with transferrin receptor. *Nature*.
448 2000;403:46-53. PMID: 10638746.
- 449 16. Bycroft C, Freeman C, Petkova D, Band G, Elliott LT, Sharp K, Motyer A,
450 Vukcevic D, Delaneau O, O'Connell J, Cortes A, Welsh S, Young A, Effingham M,
451 McVean G, Leslie S, Allen N, Donnelly P, Marchini J. The UK Biobank resource
452 with deep phenotyping and genomic data. *Nature*. 2018;562:203-209. PMID:
453 30305743.
- 454 17. Lebron JA, Bjorkman PJ. The transferrin receptor binding site on HFE, the
455 class I MHC-related protein mutated in hereditary hemochromatosis. *J Mol*
456 *Biol*. 1999;289:1109-1118. PMID: WOS:000081196100033.
- 457 18. Dickson SP, Wang K, Krantz I, Hakonarson H, Goldstein DB. Rare variants
458 create synthetic genome-wide associations. *PLoS Biol*. 2010;8:e1000294.
459 PMID: 20126254. PMCID: PMC2811148
460